Chemical Engineering Journal 155 (2009) 483–492

Contents lists available at ScienceDirect

Chemical Engineering Journal

journal homepage: www.elsevier.com/locate/cej

One-step synthesis of fine $SrTiO_3$ particles using $SrSO_4$ ore under alkaline hydrothermal conditions

Y.M. Rangel-Hernandez [a], J.C. Rendón-Angeles [a,d,*], Z. Matamoros-Veloza [b], M.I. Pech-Canul [a], S. Diaz-de la Torre [c], K. Yanagisawa [d]

[a] Research Center for Advanced Studies of the NPI, Dep. Ceramic Engineering, Saltillo-Campus, Ramos Arizpe, 25900, Coah., Mexico
[b] Saltillo Institute of Technology, Dep. Metal-Mechanics, Saltillo, 25820, Coah., Mexico
[c] Research Institute for Technology Innovation, CIITEC-IPN, Azcapotzalco 02250, Mexico
[d] Research Laboratory of Hydrothermal Chemistry, Kochi University, Kochi 780-8520, Japan

ARTICLE INFO

Article history:
Received 17 March 2009
Received in revised form 29 June 2009
Accepted 2 July 2009

Keywords:
Hydrothermal synthesis
Solid–liquid reaction
$SrTiO_3$
Celestite
Dissolution–precipitation mechanism
Kinetics

ABSTRACT

The employment of mineral $SrSO_4$ crystals and powders for preparing $SrTiO_3$ compound was investigated, with coexistence of $Ti(OH)_4{\cdot}4.5H_2O$ gel under hydrothermal conditions, at various temperatures (150–250 °C) for different reaction intervals (0.08–96 h) in KOH solutions with different concentrations. The complete dissolution of the $SrSO_4$ crystal occurred at 250 °C for 96 h in a 5 M KOH solution, resulting in the synthesis of $SrTiO_3$ particles with two different shapes (peanut-like and cubic). In contrast, very fine $SrTiO_3$ pseudospherical particles were crystallized when $SrSO_4$ powders were employed as precursor. Variations on the $SrTiO_3$ particle shape and size were found to be caused by the differences in the dissolution rate of the $SrSO_4$ phase in the alkaline KOH solution. The crystallization of $SrTiO_3$ particles was achieved by a bulk dissolution–precipitation mechanism of the raw precursors, and this mechanism was further accelerated by increasing the reaction temperature and concentration of the alkaline media. Kinetic data depicted that the activation energy required for the formation of $SrTiO_3$ powders from the complete consumption of a $SrSO_4$ single crystal plate under hydrothermal conditions, is 27.9 kJ mol^{-1}. In contrast, when $SrSO_4$ powders were employed (28–38 μm), the formation of $SrTiO_3$ powder proceeded very fast even for a short reaction interval of 3 h at 250 °C in a 5 M KOH solution.

1. Introduction

Strontium titanate ($SrTiO_3$) with perovskite structure has been widely studied because of its functional dielectric and ferroelectric properties [1–3]. $SrTiO_3$ has a wide variety of electronic applications, which include random access memory devices, oxygen sensors, actuators and electrooptical devices. Most of these applications are based on its high dielectric constant, and low temperature coefficient of dielectric constant [2–4]. Traditionally, $SrTiO_3$ powders have been prepared using $SrCO_3$ and TiO_2 by solid-state reaction at a temperature range between 900 and 1000 °C [5]. In contrast, chemical synthesis processes, namely sol–gel [2,6], chemical coprecipitation [7] and combustion synthesis [8–10], have proved to be more suitable for the preparation of well crystallized $SrTiO_3$ fine particles with very low impurity levels. However, the gel produced by chemical processes requires high temperatures to produce the crystallization of stable oxide phases, which in consequence produces a marked particle agglomeration, thus, monodispersed particles are subsequently produced by ball milling.

On the other hand, the hydrothermal synthesis is an alternative chemical synthesis route that allows the preparation of fine particles of perovskite ceramic powders free of contaminants, including $SrTiO_3$ [9–14]. This is a soft solution processing that achieves in situ nucleation and controlled growth of shaped and nanosized particles for very shorter treatment intervals, nearly two orders of magnitude than the typical solid-state reaction [9]. Furthermore, the optimization of the hydrothermal synthesis parameters and the type of aqueous solutions can lead to control the morphology, size and level of agglomeration of perovskite oxide particles [15–17]. In general, the hydrothermal synthesis of perovskite $SrTiO_3$ particles with controlled morphologies and size has recently been the subject of research [5,15–17]. Under hydrothermal conditions, the synthesis of $SrTiO_3$ has been widely conducted by employing $Ti(OH)_4$ gel (here after referred as Ti-gel). This Ti-gel is normally prepared using reagent grade chemicals, such as organometallic Ti compounds or $TiCl_4$ [15–17], while several strontium soluble salts had been used as a source of Sr^{2+} ions. Furthermore, the formation of secondary phases, namely, $SrCO_3$ is normally avoided by employing

* Corresponding author at: Research Center for Advanced Studies of the NPI, Dep. Ceramic Engineering, Saltillo-Campus, Ramos Arizpe, 25900, Coah., Mexico. Tel.: +52 844 438 9600x9672; fax: +52 844 438 9600x9610.
E-mail address: jcarlos.rendon@cinvestav.edu.mx (J.C. Rendón-Angeles).

1385-8947/$ – see front matter © 2009 Elsevier B.V. All rights reserved.
doi:10.1016/j.cej.2009.07.024

CO_2 free alkaline solutions. Moreover, the challenge for employing low grade chemical reagent precursors for preparing $SrTiO_3$ particles has not been considered yet. Thus, some minerals phases, like celestite $SrSO_4$ containing a low grade of impurity elements could be considered as precursor for preparing $SrTiO_3$ powders under hydrothermal conditions. The employment of a low cost precursor may be an additional advantage in order to propose an economical effective processing approach.

Recently, some of the present authors have been conducting exhaustive efforts in order to establish a hydrothermal synthesis route, where the main source ($SrSO_4$ celestite ore) used as precursor for the preparation of high pure strontium inorganic compounds. This processing route involves a dissolution–recrystallization mechanism which takes place and promotes the conversion of natural ores at the earth's crust into particular inorganic compounds. Hitherto, the preparation of $SrCO_3$ or SrF_2 polycrystals from the conversion of $SrSO_4$ crystal plates was found to proceed in a single reaction step in highly concentrated CO_3^{2-} and F^- hydrothermal fluids at low temperature (150–250 °C) [18,19]. Likewise, large acicular $Sr(OH)_2$ single crystals were produced by a complete dissolution of $SrSO_4$ crystal plates, the $Sr(OH)_2$ single crystals were prepared employing highly concentrated KOH solutions (5 or 10 M) at temperatures below 250 °C under hydrothermal conditions [19]. Additionally, strontium hexaferrite ($SrFe_{12}O_{19}$) functional ceramic was recently prepared by coprecipitation method, after a preliminary step that involved the leaching of mineral celestite powders [20].

According to the former literature, research works related with the synthesis of $SrTiO_3$ from celestite $SrSO_4$ ore using the hydrothermal method have not been conducted yet. Hence, in the present study we have aimed at investigating the feasibility for employing $SrSO_4$ crystalline plates and powders as a source of Sr^{2+} for the synthesis of $SrTiO_3$ powders under alkaline hydrothermal conditions. Preliminary attempts were made to optimize the experimental conditions (temperature, time and concentration of the KOH alkaline media) required for the single-step synthesis of the perovskite $SrTiO_3$ powders from the $SrSO_4$ ore. Additionally, details regarding the reaction pathway and the morphology of the synthesized products are discussed in terms of the reactivity of the $SrSO_4$ in the hydrothermal KOH fluids.

2. Experimental procedure

2.1. Materials preparation

A crystalline aggregate celestite ($SrSO_4$) ore was collected from an area placed at Northeast Mexico (Coahuila State). Small $SrSO_4$ single crystal plates were obtained by cutting the large aggregate specimens in a parallel direction to the cleavage plane (0 0 1) with a diamond disk, obtaining square plates with dimensions of 6 ± 1 mm side and 2 ± 0.5 mm thick. The plates were washed with deionized water and ultrasonically cleaned. A preliminary X-ray powder analysis of the selected celestite specimen (Fig. 1) revealed that the mineral belongs to the orthorhombic system with *Pnma* space group (JCPD card 05-0593) and unit cell parameters: $a = 8.3628 \pm 0.0004$ Å, $b = 5.3511 \pm 0.0004$ Å, $c = 6.8675 \pm 0.0004$ Å. The "*a*" and "*c*" cell parameters calculated are slightly different from those determined for a pure $SrSO_4$ sample ($a = 8.359$ Å, $b = 5.352$ Å and $c = 6.866$ Å, JCPD card 05-0593) with a very low content of impurities, <0.11 wt.%; such as Ba < 0.1 wt.%, Na < 0.01 wt.%, Al < 0.001 wt.%. In particular, the enlargement of the unit cell parameters "*a*" and "*c*" of the $SrSO_4$ sample employed for the experiments in the present work, is attributed to the incorporation of a large amount of Ba^{2+} ions. Indeed, wet chemical analyses of the $SrSO_4$ crystal plates showed that the major

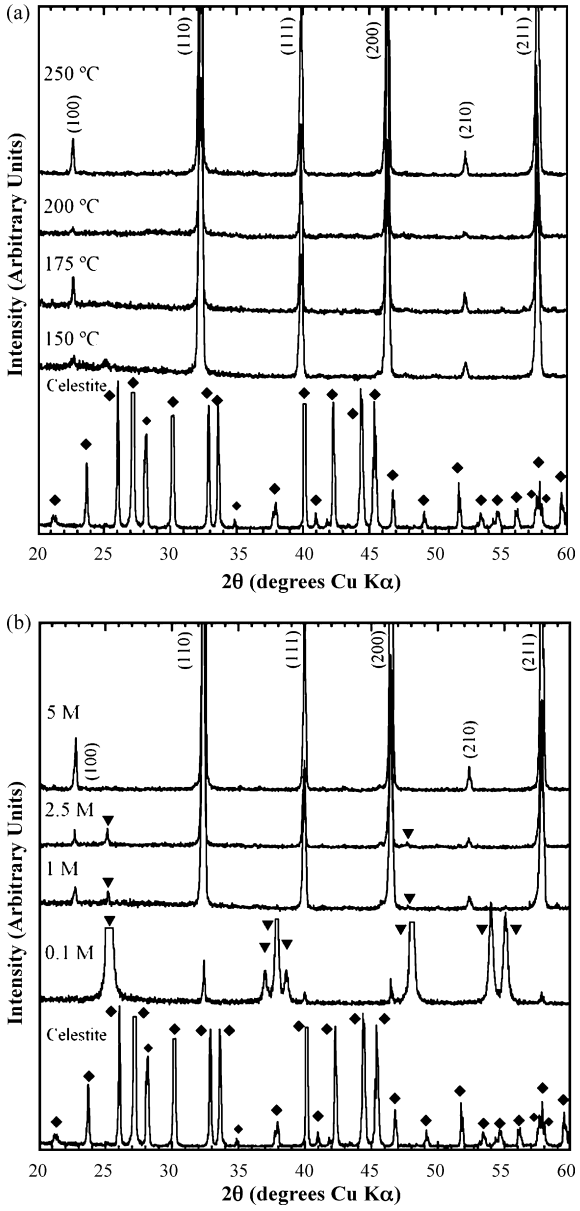

Fig. 1. XRD patterns of the reaction products obtained after the hydrothermal treatment of celestite crystals conducted for 96 h at an autoclave filling ratio of 40%, (a) in a 5 M KOH solution at different temperatures and (b) at 250 °C with different concentrations of the KOH solution. Miller indexes correspond to $SrTiO_3$ with perovskite cubic structure. (♦) Celestite ore ($SrSO_4$) and (▼) anatase (TiO_2).

constituents are Sr = 42.97 wt.%, Ba = 5.67 wt.%, SO_4^{2-} = 50.11 wt.% and CO_3^{2-} = 0.60 wt.%, which corresponds to $SrSO_4$ = 88.3 wt.%, $BaSO_4$ = 9.6 wt.% and $SrCO_3$ = 1.5 wt.%. Other minor impurities with a content <0.6 wt% were Ca, Na, Fe and K.

Titanium hydroxide gel (Ti-gel) which was selected as a Ti source, was preliminary prepared by the following procedure. A 1 M $TiCl_4$ solution (150 ml) prepared by dissolving $TiCl_4$ in ice-cold water was poured into 5 M NaOH solution (500 ml), which resulted in the formation of a white precipitate [16]. The precipitate was then filtered and washed for three times under stirring with CO_2 free water at 50 °C. Finally the pasty Ti-gel was obtained by centrifuge to remove water. The chemical formula of the precursor gel was determined by thermal gravimetric analyses (TG/DTA SEIKO model SSC5200) conducted in air up to 1000 °C at a heating rate of 5 °/min. Thus, the chemical formula of the as prepared Ti-gel was determined to be $Ti(OH)_4{\cdot}4.5H_2O$.

2.2. Hydrothermal treatments

A $SrSO_4$ single crystal plate (0.2 g) and a selected amount of freshly prepared Ti-gel were placed at the bottom of a Teflon-lined stainless steel vessel. To control the molar Sr/Ti ratio incorporated for each run inside the vessel, three different weight $SrSO_4$/Ti-gel ratios of 0.4, 0.2 and 0.08 which correspond to the molar Sr/Ti ratios of 2, 1 and 0.4, respectively, were employed. Additionally, a different set of experiments were conducted by using the same amount (0.2 g) of $SrSO_4$ powder with a particle size between 25 and 38 μm. The powder was produced by milling the $SrSO_4$ crystals (50 g) in zirconium milling media for 1 h and subsequently sieved using stainless steel meshes of 400 (38 μm) and 500 (25 μm). Hydrothermal treatments were conducted by employing a KOH alkaline solution with different concentrations (0.1, 1, 2.5 and 5 M), and all the runs were conducted at a constant filling of 40 % of the inner vessel volume (27 ml). The autoclaves were sealed and placed in a forced-air convection oven, which was then heated up to a predetermined temperature (150–250 °C). The vessels were held at each temperature for several reaction intervals (0.08–96 h). After the hydrothermal treatment, the reaction products were separated from the remaining solution, and ultrasonically washed with deionized water.

2.3. Characterization

X-ray powder diffraction analyses were employed to determine the crystalline phases of the reaction products by using a X-ray diffractometer (Rigaku RTP-300RC) with graphite-monochromatized Cu Kα radiation (λ = 1.54056 Å) at 40 kV and 100 mA. Diffraction patterns were collected in the 10–70° 2θ range, at a scanning speed of 4°/min in a 2θ/θ scanning mode with a 0.02° step. Lattice parameter "***a***" was calculated by the least square method, using Si as an internal standard. The morphology of the particles was observed by scanning electron microscopy (Phillips XL30 ESEM), and simultaneously the Sr and Ti atomic content was calculated from an average of 10 punctual microprobe analyses conducted by X-ray energy dispersive equipment. In addition, the particle size was estimated from SEM images of 100 particles.

The kinetics related with the consumption of $SrSO_4$ crystals and the simultaneous formation of $SrTiO_3$ powders was evaluated considering the shrinking core model for solid–liquid systems reported elsewhere [21,22], because it involves the bulk solid dissolution in a liquid phase, similar to the chemical reaction proposed to achieve the transformation of $SrSO_4$ into $SrTiO_3$ in the current study. The model considers that the reaction rate "*r*" of the solid $SrSO_4$ crystal plate could be controlled by the surface chemical reaction or the reactant diffusion through the solution boundary layer, and as a function of the consumption ratio "α", can be written as

$$r = \frac{d\alpha}{dt} = kf(\alpha) \quad (1)$$

while, the solid crystal plate ($SrSO_4$) consumption, α, is given by the following expression:

$$\alpha = \frac{C_{0SrSO_4} - C_{SrSO_4}}{C_{0SrSO_4}} \quad (2)$$

where C_{0SrSO_4} and C_{SrSO_4} represent in this study the amount of $SrSO_4$ in the original crystal plate and that in the remained crystal after each hydrothermal treatment conducted in a 5 M KOH solution, respectively. The consumption ratio (α) for each experimental run was obtained from the molar $SrSO_4$ content on both the original crystal and remained crystal, before and after the hydrothermal treatment, respectively. These molar $SrSO_4$ contents were calculated using the concentration of $SrSO_4$ determined by ICP in the raw $SrSO_4$ crystals and the $SrSO_4$ crystal weights measured before and after each treatment, respectively.

Thus, the rate constant "*k*" was determined from linear regression of the experimental data portrayed in $\ln(1-\alpha)$ vs. *t* graphs. This particular way considers empirical kinetic laws of the type $f(\alpha) = (1-\alpha)^n$ where *n* is a reaction order. This expression allows calculating a series of functions which can predict empirically the kinetics and mechanism associated with a chemical reaction between the solid and liquid. In the present work, the rate constants "*k*" were calculated by the first order kinetics, this function was found to fit well the experimental data among other equations related with the dissolution kinetics of solid–liquid systems, which also were evaluated [21]. Finally, the activation energy "E_a" was calculated by the Arrhenius equation using linear regression. This activation energy in the current system is associated with the $SrSO_4$ and hydrous Ti-gel bulk dissolution in the alkaline solution, which allows the synthesis of $SrTiO_3$ powders in the current system.

3. Results and discussion

In a preliminary approach, the experiments were directed towards to establish the morphological details associated with the chemical reaction of $SrSO_4$ crystal plates and the synthesis of $SrTiO_3$, in order to probe whether this reaction could proceed by the pseudomorphic conversion mechanism [18,19]. Hence, the hydrothermal treatments were conducted at the following experimental conditions: temperature of 250 °C, reaction interval of 96 h in a 5 M KOH solution with three different molar Sr/Ti-gel ratios of 2, 1 and 0.4; samples ID CT5, CT6 and CT7 in Table 1, respectively. After the hydrothermal treatments, the appearance of the remaining solid products in the autoclave was different depending on the molar Sr/Ti-gel ratio. The partially reacted celestite crystal remained at the autoclave bottom, when the reaction was not completed at a molar Sr/Ti of 2. Likewise, the pasty Ti-gel remained when the smallest molar Sr/Ti ratio (0.4) was employed. Both solid products were easily recovered from the Teflon liner bottom using tweezers. In these experiments a second reaction product consisting on fine particles was also obtained, and these particles were washed with plenty of water and collected by centrifugation. These results indicate that the transformation of the $SrSO_4$ crystals derives on the synthesis of the $SrTiO_3$ compound, but without proceeding by a pseudomorphic conversion process [18,19].

3.1. Structural crystalline features of the $SrTiO_3$ powders

In Table 1 are summarized the treatment experimental conditions together with the crystalline phases identified as major reaction products and remaining raw precursors. Typical XRD patterns of the reaction products (white powders) obtained by hydrothermal treatments conducted using $SrSO_4$ crystals for 96 h in a 5 M KOH solution at different temperatures are shown in Fig. 1a. The diffraction peaks of the major reaction product produced were indexed with that of $SrTiO_3$ (space group $Pm\bar{3}m$, JCPDS card 35-0734). The formation of the $SrTiO_3$ powder occurred at a temperature as low as 150 °C; at this temperature, few traces of TiO_2 (tetragonal structure, anatase, JCPDS card 86-1156) were produced as a by-product. However, when the treatments were conducted at temperatures below 200 °C, small pieces of the original $SrSO_4$ crystal and Ti-gel paste together with the $SrTiO_3$ powder were found at the Teflon liner bottom (see Table 1). The $SrSO_4$ crystal chunk and the small pasty gel piece were removed from the Teflon chamber using plastic tweezers, once the $SrTiO_3$ powder was gravimetrically separated. Thus, the remaining raw precursors ($SrSO_4$ crystal chunk and small piece of Ti-gel) were not included in the powder samples used for the X-ray diffraction analyses. The complete consumption of the $SrSO_4$

Table 1
Summary of the hydrothermal treatments conducted for studying the conversion of $SrSO_4$ crystals or powders into $SrTiO_3$.

Sample	Mineralizer KOH (M)	Molar ratio Sr/Ti	Temperature (°C)	Duration (h)	Determined reaction products	Lattice parameter a (Å)	Cell volume (Å^3)	Element content determined by EDS	
								Sr^{2+} (at.%)	Ti^{4+} (at.%)
CT1	0.1	1	250	96	$SrSO_4$, TiO_2[b], $SrTiO_3$, Ti-gel,	–	–	–	–
CT2	1	1	250	96	$SrTiO_3$, $SrSO_4$, Ti-gel	3.9067 ± 0.0002	59.627 ± 0.007	50.82 ± 0.50	49.18 ± 0.50
CT3	2.5	1	250	96	$SrTiO_3$, $SrSO_4$, Ti-gel	3.8996 ± 0.0005	59.301 ± 0.022	50.52 ± 0.40	49.48 ± 0.40
CT4	5	1	250	96	$SrTiO_3$	3.9001 ± 0.0010	59.327 ± 0.049	50.93 ± 0.90	49.07 ± 0.90
CT5	5	2	250	96	$SrTiO_3$, $SrSO_4$,	3.9050 ± 0.0008	59.547 ± 0.029	49.86 ± 0.70	50.14 ± 0.70
CT6	5	0.4	250	96	Ti-gel, $SrTiO_3$, $SrCO_3$	3.8974 ± 0.0011	59.200 ± 0.050	–	–
CT7	5	1	200	96	$SrTiO_3$, $SrSO_4$, Ti-gel	3.9050 ± 0.0006	59.548 ± 0.025	–	–
CT8	5	1	175	96	$SrTiO_3$, $SrSO_4$, Ti-gel	3.9027 ± 0.0009	59.444 ± 0.030	–	–
CT9	5	1	150	96	$SrTiO_3$, $SrSO_4$, Ti-gel, TiO_2[b]	3.9057 ± 0.0010	59.581 ± 0.049	–	–
CT10	5	1	250	6	$SrSO_4$, Ti-gel, TiO_2[b], $SrTiO_3$, $SrCO_3$	3.9077 ± 0.0006	59.673 ± 0.025	–	–
CT11	5	1	250	12	$SrSO_4$, TiO_2, Ti-gel, $SrTiO_3$	3.9049 ± 0.0007	59.547 ± 0.028	48.51 ± 0.90	52.49 ± 0.90
CT12	5	1	250	24	$SrTiO_3$, $SrSO_4$, TiO_2[b], Ti-gel	3.9034 ± 0.0010	59.475 ± 0.049	–	–
CT13	5	1	250	48	$SrTiO_3$, $SrSO_4$, TiO_2[b], Ti-gel	3.9011 ± 0.0009	59.371 ± 0.030	49.03 ± 0.90	50.97 ± 0.90
PT1[a]	5	1	250	0.08	$SrSO_4$, TiO_2[b], Ti-gel, $SrTiO_3$	3.9055 ± ±0.0009	59.571 ± 0.030	–	–
PT2[a]	5	1	250	0.75	$SrTiO_3$	3.9099 ± 0.0001	59.771 ± 0.005	50.90 ± 0.70	49.10 ± 0.70
PT3[a]	5	1	250	3	$SrTiO_3$	3.9030 ± 0.0009	59.460 ± 0.030	50.29 ± 0.10	49.71 ± 0.10
PT4[a]	5	1	250	24	$SrTiO_3$	3.9064 ± 0.0006	59.613 ± 0.025	50.19 ± 0.20	49.81 ± 0.20
Strontium titanate ($SrTiO_3$)[c]						3.905	59.550	50.0	50.0

[a] Treatments conducted using $SrSO_4$ mineral powder as a precursor of Sr^{2+}.
[b] TiO_2, anatase system, JCPDS card No. 86-1156.
[c] Strontium titanate (Tousinite), JCPDS card No. 35-0734.

Fig. 2. XRD patterns of the reaction products obtained after the hydrothermal treatment of $SrSO_4$ mineral powders conducted at 250 °C in a 5 M KOH solution at an autoclave filling ratio of 40% for several reaction intervals. Miller indexes correspond to $SrTiO_3$ with perovskite cubic structure. (♦) Celestite ore ($SrSO_4$), (▼) anatase (TiO_2).

crystal plate which results in the synthesis of $SrTiO_3$ compound by-product free, was found to occur by the reaction at 250 °C for 96 h in a 5 M KOH solution. The formation of the crystalline $SrTiO_3$ phase was observed to occur even at very short reaction intervals of 6 h at 250 °C, but the complete reaction of the $SrSO_4$ crystal into $SrTiO_3$ was achieved at a longer reaction interval of 96 h.

On the other hand, in order to investigate the effect of the concentration of the alkaline solution on the synthesis of $SrTiO_3$ by using $SrSO_4$ crystals, a series of hydrothermal treatments were conducted at 250 °C for 96 h, employing different concentrations of the KOH solution. When hydrothermal treatments were conducted in a low concentrated KOH solution (0.1 M), a predominant formation of TiO_2 compound with anatase structure was found to occur, as shown in Fig. 1b. And a small amount of the $SrTiO_3$ phase was also found in the reaction products, as suggested by the (1 1 0) Miller index peak of $SrTiO_3$. The presence of TiO_2 in the reaction products was further limited by increasing the concentration of the KOH solution up to 5 M. Thus, when the hydrothermal treatments were conducted in a 5 M KOH solution, only the $SrTiO_3$ crystalline phase was found in the reaction products. Therefore, the concentration of the alkaline solution is the factor that plays an important role in order to reach the optimum conditions for dissolving both raw precursors ($SrSO_4$ crystal and Ti-gel) to synthesize the $SrTiO_3$ particles, when compared with the reaction temperature and time.

Fig. 2 shows typical X-ray powder diffraction patterns of the products obtained from the hydrothermal treatments conducted at 250 °C in 5 M KOH by using raw $SrSO_4$ powders (particle size 25–38 μm) for various reaction intervals. In contrast with those experiments conducted using $SrSO_4$ crystals, when the source of strontium (celestite) was incorporated as powder, the pasty Ti-gel was not found in the reaction product obtained even for the shortest reaction interval of 0.08 h. Likewise, the X-ray powder diffraction results also demonstrate that the reactivity of the $SrSO_4$ was further accelerated with the incorporation of the celestite powder. Hence, the formation of the new $SrTiO_3$ phase was found to proceed at a short reaction interval of 0.08 h. At intermediate stages of the reaction (0.25–0.75 h), the major constituent found in the reaction products was $SrTiO_3$; however, a small amount of the raw $SrSO_4$ particles and TiO_2 was also detected. These crystalline phases

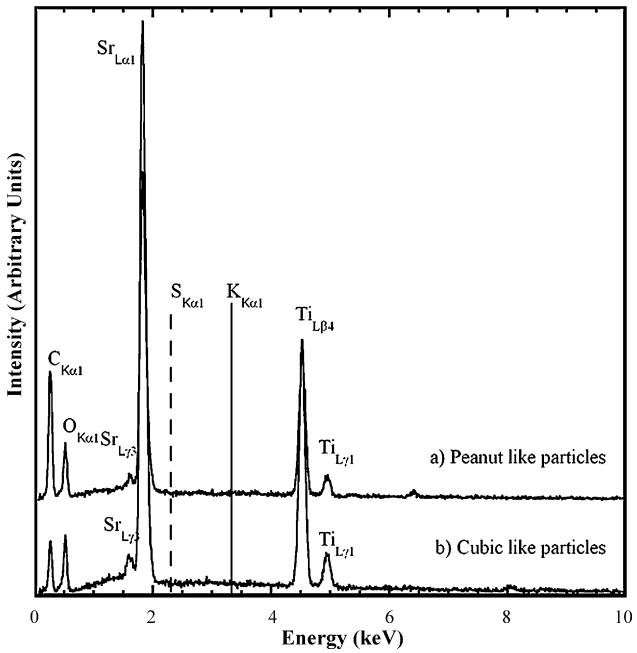

Fig. 3. EDX spectra of $SrTiO_3$ (a) peanut-like and (b) cubic particles obtained under hydrothermal conditions at 250 °C for 96 h in a 5 M KOH solution.

were gradually dissolved in the solution to complete the formation of $SrTiO_3$, which proceeded at a reaction interval of 24 h. In addition, the values of the lattice parameter "***a***" of the cubic perovskite structure ABO_3, which was determined for those products obtained at some selected experimental conditions given in Table 1, revealed that those of the obtained $SrTiO_3$ particles closely resembles the lattice parameter "***a***" of the $SrTiO_3$ compound (3.905 A, JCPDS card 35-0734). The chemical composition determined by electron microprobe analyses of the products obtained as a $SrTiO_3$ single phase, revealed that they have an average Sr:Ti molar ratio of 50.4 (4):49.6 (4), which is similar to the stoichiometric Sr:Ti molar ratio of 50:50 of $SrTiO_3$. Additionally, the EDX spectra of the $SrTiO_3$ powders obtained for 96 h at 250 °C in a 5 M KOH solution (Fig. 3), showed that the incorporation of impurities inside the crystalline perovskite $SrTiO_3$ structure was further limited, because traces of barium, sulfur or potassium incorporated in the system were not detected on the EDX spectra shown in Fig. 3. Thus, these results indicate that the release of major impurities [19], namely Ba^{2+}, is simultaneously achieved during the synthesis of $SrTiO_3$ powders derived from using the mineral $SrSO_4$ crystal as a raw reagent.

3.2. Morphological aspects of the hydrothermally synthesized $SrTiO_3$ powders

Typical morphological aspects of the reaction products are shown in Fig. 4. The observations conducted by SEM revealed that when the $SrSO_4$ crystals were treated for 96 h in a 5 M KOH solution for different temperatures, $SrTiO_3$ particles with a bimodal size distribution were obtained due to the complete consumption of the $SrSO_4$ crystal. In general, the $SrTiO_3$ powders produced at 200 °C are constituted by a large amount of agglomerated irregular particles with peanut-like shape (Fig. 4a); the length and width of these particles are in the range of 0.5–1 μm and 0.2–0.5 μm, respectively. A small amount of bulky crystals with a regular pseudocubic shape and a particle size in the range of 1–4 μm was also found in the reaction products. An increase in the temperature up to 250 °C leads to crystal growth of either peanut-like shape (length = 1–5 μm and width = 0.5–1 μm) or pseudocubic (3–6 μm) $SrTiO_3$ particles, as shown in Fig. 4b. Furthermore, a relative increase in the amount of pseudocubic particles was found to occur by increasing the treatment temperature. From these results, it is expected that the particle growth observed for the peanut-like and pseudocubic shaped particles takes place by the Ostwald ripening particle coarsening mechanism [23]. This inference is suggested by the fact that the small sized peanut-like particles produced at lower temperatures (<200 °C), were not observed in the $SrTiO_3$ powder obtained at 250 °C. Another point that deserves to be emphasized is that related with the structural features of either peanut-like or cubic-like shaped particles. EDX spectra obtained on both particles did not show a marked difference on the molar Sr/Ti ratio, because the particles contain similar Sr and Ti amounts as it is suggested by the corresponding EDX spectrum in Fig. 3. Hence, these results are in good agreement with the X-ray diffraction and demonstrate that both peanut and cubic shaped particles belong to the crystalline structure of $SrTiO_3$.

On the other hand, the SEM images (Fig. 5) indicate that the $SrTiO_3$ particle size and shape are markedly influenced by the concentration of the KOH solution (hydrothermal fluid). The micrographs in Fig. 5 correspond to $SrTiO_3$ powders obtained by hydrothermal treatments using $SrSO_4$ crystals at 250 °C for 96 h. In general, a large amount of agglomerated bulky pseudocubic $SrTiO_3$ particles, with a particle size ranging from 5 to 15 μm, together with a small amount of cubic monodispersed irregular particles (particle size of 1–3 μm), were preferentially crystallized when KOH solutions with a concentration below 2.5 M were used (Fig. 5a and b). In contrast, a reduction in the particle size of the bulky pseudocubic particles, as well as the presence of peanut-like shaped particles, occurred when a highly concentrated KOH solution (5 M) was employed for the hydrothermal treatment (Fig. 5c). Hitherto, it has been found that under hydrothermal conditions, the metal concentration and KOH solution pH are important variables for preparing single phase perovskite titanate oxides, including $SrTiO_3$ and $BaTiO_3$. The single ABO_3 phase is commonly obtained at high pH values >12, likewise, the particle morphology and size are affected by the feedstock of the KOH solution under hydrother-

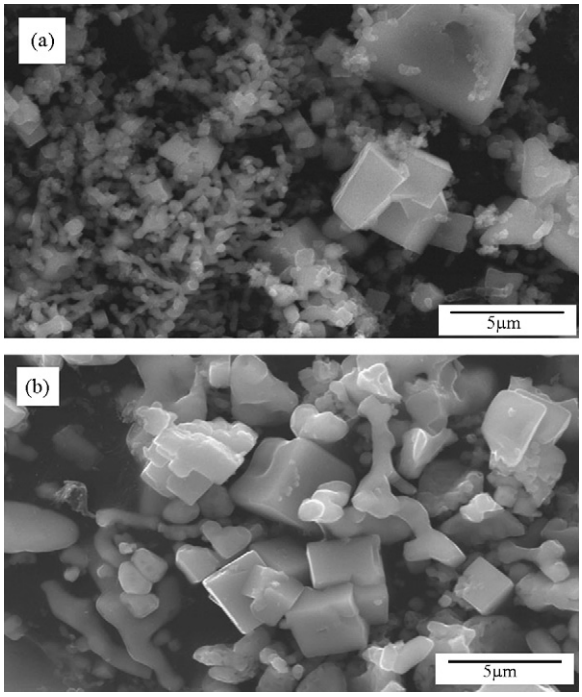

Fig. 4. SEM images of the $SrTiO_3$ particles obtained after hydrothermal treatments of the $SrSO_4$ crystal plates, conducted for 96 h in a 5 M KOH solution at temperatures of (a) 200 °C and (b) 250 °C.

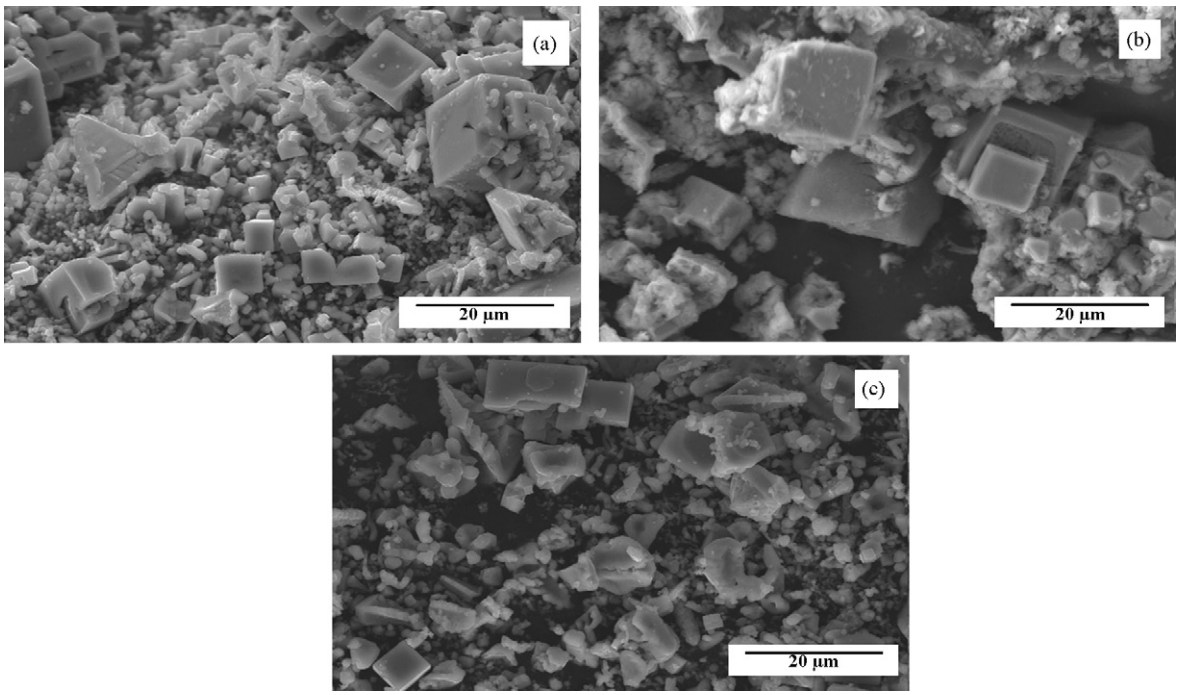

Fig. 5. SEM micrographs of the $SrTiO_3$ particles obtained after hydrothermal treatments of the $SrSO_4$ crystal plates, conducted at 250 °C for 96 h in various KOH solutions with the following concentrations: (a) 1 M, (b) 2.5 M and (c) 5 M, respectively.

mal and glycothermal conditions [24,25]. Thus, for some alkaline earth titanate oxides ($Pb_{0.7}La_{0.3}TiO_3$), the particle size decreases by increasing the feedstock concentration of the hydrothermal media. Spherical particles (0.125 μm) were preferentially crystallized under hydrothermal conditions at 220 °C in a 6 M KOH solution using a lanthanum titanate hydroxide (LTOH) precursor. In contrast, the decrease of the KOH concentration (<2 M) resulted in the formation of cubic (0.5 μm) and lamellar (0.25 μm) particles. In particular, the differences of the particle morphology were associated with the low solubility of the LTOH gel with low concentrated alkaline KOH solutions [25]. In our case, however, the differences in particle morphology and size distribution might be associated with the supersaturation rate of the hydrothermal media (KOH solution), which markedly alters the particle growth rate. Therefore, the saturation rate of the stable aqueous species of $Sr(OH)_2$ and $Ti(OH)_4{}^0$ in mild concentrated KOH solutions (1 or 2.5 M) might be lower than that reached in a more concentrated KOH solution (5 M). Thus, the growth rate of $SrTiO_3$ particles must be reduced due to the decrease on the mass transport rate of the species ($Sr(OH)_2$ and $Ti(OH)_4{}^0$) that feed the growing particles when low or mild concentrated alkaline solutions are employed.

Moreover, a marked difference in the $SrTiO_3$ particle morphology was found by hydrothermal treatments of $SrSO_4$ powders at 250 °C in a 5 M KOH solution for different reaction intervals. Fig. 6 shows a typical aspect of the morphology of the $SrTiO_3$ particles obtained at various reaction intervals. In general, the use of $SrSO_4$ powders with a narrow particle size distribution in the range from 25 to 38 μm, favored the crystallization of very fine cubic $SrTiO_3$ particles, even at very short reaction intervals (0.08 h, Fig. 6a). However, a bimodal size distribution was observed for this $SrTiO_3$ powder, which consisted of a large amount of pseudocubic particles with an average size of 0.75 μm and a very small amount of large cubes of 1.5 μm in size. These two different particle morphologies were observed for the $SrTiO_3$ powder after the hydrothermal treatment for 1 h (Fig. 6b), thus, the $SrTiO_3$ powder is constituted by very fine particles (average size of 0.25 μm) with semi-spherical shape and a few amount of small (average size of 1.0 μm) pseudocubic particles. In contrast, at the longest reaction interval of 24 h, the preferential formation of very fine pseudospherical $SrTiO_3$ particles with an average particle size of 0.4 μm was observed. These particles exhibit a homogeneous particle size distribution in comparison with that determined for the $SrTiO_3$ powders obtained at short reaction intervals (<3 h). In general, the cubic or pseudocubic morphologies resemble the crystallographic nature of the pseudocubic perovskites produced by hydrothermal synthesis [26]. Thus, the formation of the cubic particles is expected to be achieved by a crystallographic habit growth, which proceeded when the alkaline solution reaches a supersaturation steady-state with the species $Sr(OH)_2$ and $Ti(OH)_4{}^0$. And a massive homogeneous nuclei formation and fast growth of the cubic particles might occur in the hydrothermal system for reaction intervals less than 3 h. However, the $SrTiO_3$ cubic particles produced at early stage underwent into a preferential dissolution by increasing the reaction interval. The particle dissolution mainly occurs at high energy faceted edges of the cubic particles, because the $SrTiO_3$ particles obtained at 1 h do not show well defined edges (Fig. 6b), but a few small particles still retain their cubic shape [26]. At the final stage of growth (24 h, Fig. 6c), the cubic particles are further dissolved and the pseudospherical shaped particles were reprecipitated from the solution.

3.3. *Synthesis of $SrTiO_3$ powders via the hydrothermal transformation of $SrSO_4$*

Among the reactions reported for celestite ($SrSO_4$), the use of strontium ore to produce strontium titanate ($SrTiO_3$) in a single-step reaction under alkaline hydrothermal conditions has not been studied yet [18,19,27]. Thus, the reactants, Ti-gel ($Ti(OH)_4{\cdot}4.5H_2O$) and mineral celestite (crystal) were incorporated as a source of Ti^{4+} and Sr^{2+} ionic species, together with the alkaline hydrothermal solution (KOH). Hence, the synthesis of $SrTiO_3$ powders from $SrSO_4$ crystals plates as main source of Sr^{2+}, is proposed to proceed in accordance with the chemical Eqs. (3) and (4). In general, the formation of $BaTiO_3$ particles, which is analogous to that for $SrTiO_3$ has been widely investigated under hydrothermal conditions. In par-

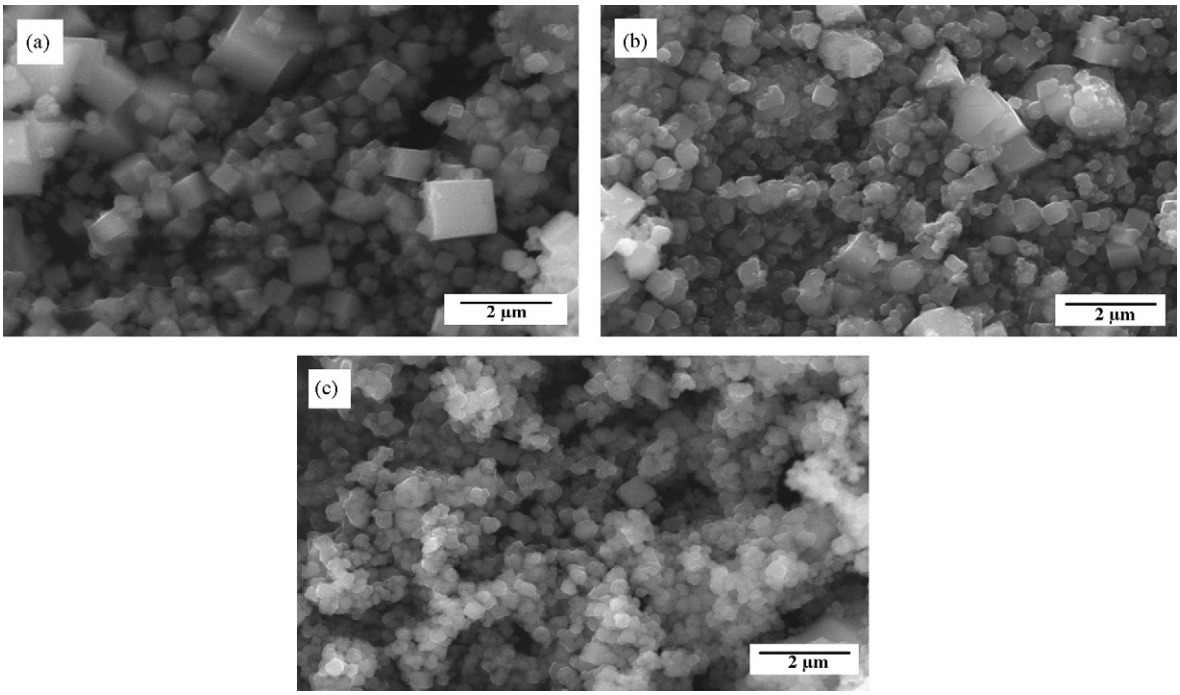

Fig. 6. SEM micrographs of the $SrTiO_3$ particles obtained after hydrothermal treatment of the $SrSO_4$ powders (25–38 μm size), conducted at 250 °C in 5 M KOH solution for reaction intervals of (a) 0.08 h, (b) 1 h and (c) 24 h.

ticular, the synthesis of these powders was found to proceed by two different reaction mechanisms, dissolution–precipitation [28–30] or in situ transformation of the raw precursors (when TiO_2 particles are used) [28,31]. The current reaction system proposed differs from those previously studied, because neither Sr^{2+} ions nor TiO_2 particles were included as reaction precursors. Hence, a coupled reaction processes that involves the dissolution of the $SrSO_4$ crystal (Eq. (3)) and the simultaneous Ti-gel dehydration process [32], are likely to lead the synthesis of the $SrTiO_3$ particles in our case.

$$SrSO_{4(crystal)} + Ti(OH)_4{\cdot}4.5H_2O_{(gel)} + 2KOH_{(aq)} \rightarrow Sr(OH)_{2(aq)} + K_2SO_{4(aq)} + Ti(OH)_{4(aq)}{}^0 + 4.5H_2O \quad (3)$$

$$Sr(OH)_{2(aq)} + Ti(OH)_{4(aq)}{}^0 \rightarrow SrTiO_{3(s)} + 3H_2O \quad (4)$$

Details of the reaction pathway that achieves the synthesis of $SrTiO_3$ from $SrSO_4$ ore crystal plates under hydrothermal conditions are shown in Fig. 7. Macroscopic aspects related with the single-step synthesis process were determined during the early stages of the reaction at 200 °C for 6 h in a 5 M KOH solution, and are shown in Fig. 7. In general, the images revealed by petrographic microscope observations, indicate that the $SrSO_4$ crystal is embedded in the Ti-gel (Fig. 7a) and in the early step the reaction proceeds by the crystal dissolution. The consumption of the $SrSO_4$ crystal proceeds locally on those surfaces exposed to the alkaline fluid and also on those crystal surfaces in contact with the Ti-gel (Fig. 7b). These observations are in a good agreement with those previously reported elsewhere [33], which provided clear evidences of the poor chemical stability of $SrSO_4$ phase in highly concentrated alkaline hydrothermal solutions (5 and 10 M NaOH). The continuous dissolution of the $SrSO_4$ crystal must result in the formation of the $Sr(OH)_2$ species (Eq. (3)), because of the high alkaline conditions of the hydrothermal media. Indeed, additional evidences that support the above inference were revealed by treating only the Ti-gel in 5 M KOH solution by the treatment conducted at 200 °C for 6 h. The pasty Ti-gel neither exhibited dissolution in the KOH solution nor crystallization into anatase pro-

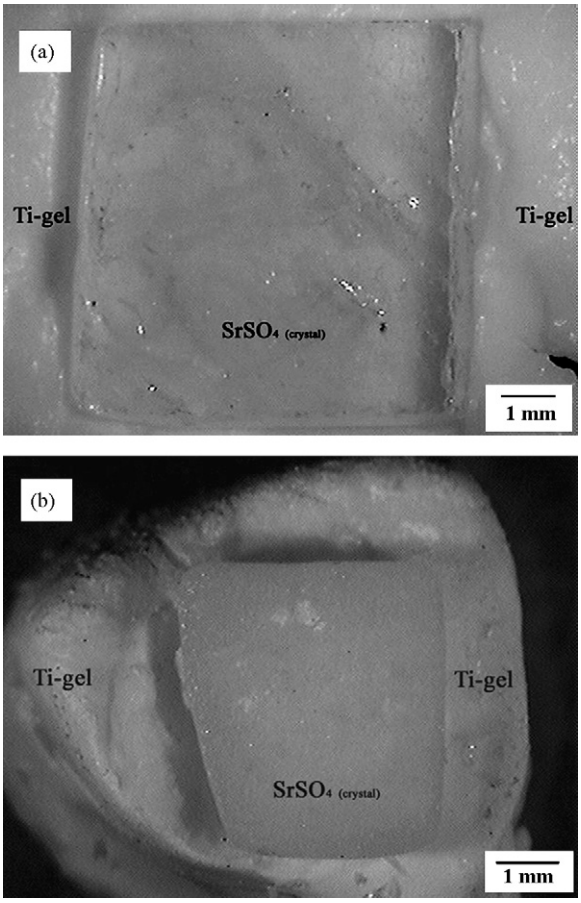

Fig. 7. Micrographs showing the macroscopic aspects of the (a) original $SrSO_4$ crystal plate embedded in the Ti-gel previous the hydrothermal treatment, and (b) the partially reacted $SrSO_4$ crystal plate and Ti-gel treated at 200 °C for 6 h in an alkaline 5 M KOH solution.

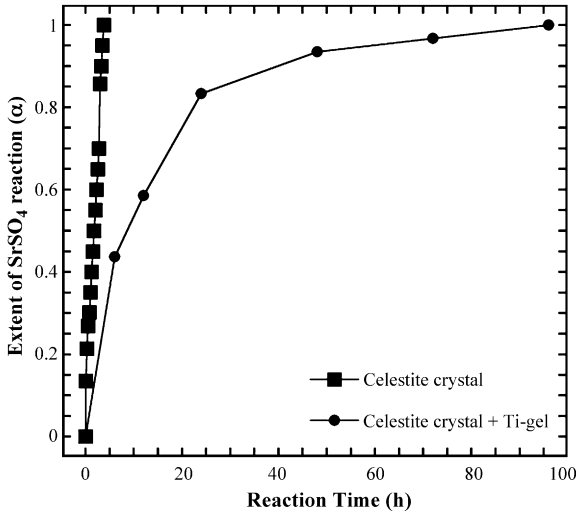

Fig. 8. Consumption curves (α) of $SrSO_4$ crystal treated under hydrothermal conditions at 250 °C for various reaction intervals in a 5 M KOH solution. Two different treatments were conducted without any Ti-gel addition (■) and in the presence of the Ti-gel (b).

ceeded. This result suggests that the solubility of the pasty Ti-gel is low in high concentrated KOH (>0.1 M) solutions, as was recently reported elsewhere [32]. However, the extent of the $SrSO_4$ crystal dissolution (α) was markedly reduced due to the presence of the pasty Ti-gel in the reaction system (Fig. 8). Hence, the Ti-gel reduces the dissolution rate of the $SrSO_4$ phase. Thus, Eq. (4) is proposed for the formation of the $SrTiO_3$ and involves the presence of the $Ti(OH)_4{}^0{}_{(aq)}$ species which is obtained by the Ti-gel dehydration process [32]. The formation of the $Ti(OH)_4{}^0$ species in the current system is supported by thermodynamic data which indicate that aqueous $Ti(OH)_4{}^0$ is the most stable phase coexisting in highly concentrated alkaline solutions in hydrothermal systems [34,35]. The nucleation and growth processes of the $SrTiO_3$ particles must proceed when the alkaline (KOH) solution reaches a supersaturation state of the species $Sr(OH)_2$ and $Ti(OH)_4$. In accordance with the experimental results, $SrTiO_3$ particles precipitation normally occurred at Ti-gel surface and in the space between the remaining $SrSO_4$ crystals, because the mass transport was limited in our experiments, which were conducted under conditions of neither agitation nor thermal gradients. The reaction concludes when the bulk dissolution of both $SrSO_4$ and Ti-gel is completed.

3.4. Kinetics of $SrSO_4$ crystal plate consumption and the $SrTiO_3$ synthesis under hydrothermal alkaline conditions

The consumption ratio (α) of $SrSO_4$ crystal plates was determined for reactions with stoichiometric molar Sr:Ti ratio of 1:1 at four temperatures in the range between 150 and 250 °C for different reaction intervals up to 96 h. The variation of the factor α related to the kinetic aspects of the consumption of $SrSO_4$ and the formation of $SrTiO_3$ is given in Fig. 9. In general, the reaction proceeded rapidly only in those crystals treated above 200 °C for reaction intervals up to 24 h; then, the rate of dissolution was slightly slowed down by increasing the reaction interval over 48 h. The present results indicate that under these conditions a large consumption ratio of the $SrSO_4$ crystal, which reaches a 60% (α = 0.6) yield proceeds rapidly at a relatively low temperature (200 °C). However, the rate of consumption higher than 95% (α = 0.95) was achieved only for the longest reaction interval (96 h) at temperatures above 200 °C (Fig. 9a). Likewise, the consumption rate "α" was markedly accelerated by increasing the KOH solution concentration up to 5 M, and led to a complete consumption (α = 1) at 250 °C for 96 h, while the treatments conducted in mild concentrated KOH solutions (<2.5 M) yielded only a dissolution rate of 90% (α = 0.9) (Fig. 9b). Nowadays, the Johnson–Mehl–Avrami or the population balance models have been used for the treatment of chemical kinetic data corresponding to the nucleation and growth process of $BaTiO_3$ particles under hydrothermal conditions [26,36,37]. However, the application of each model is critically limited by selecting some experimental conditions that favor an homogeneous nuclei formation and particle growth, such as mixing and homogeneous distribution of reactants (Sr^{2+} and Ti-gel), temperature, pH and concentration of the alkaline solution. In contrast, among the kinetic functions, in particular those based on the theory of solid–liquid chemical reactions, are those which that experimentally resemble the kinetics of the current synthesis process investigated. This is because the experimental data are related with the chemical dissolution of solid species ($SrSO_4$ crystal and Ti-gel), which simultaneously promotes

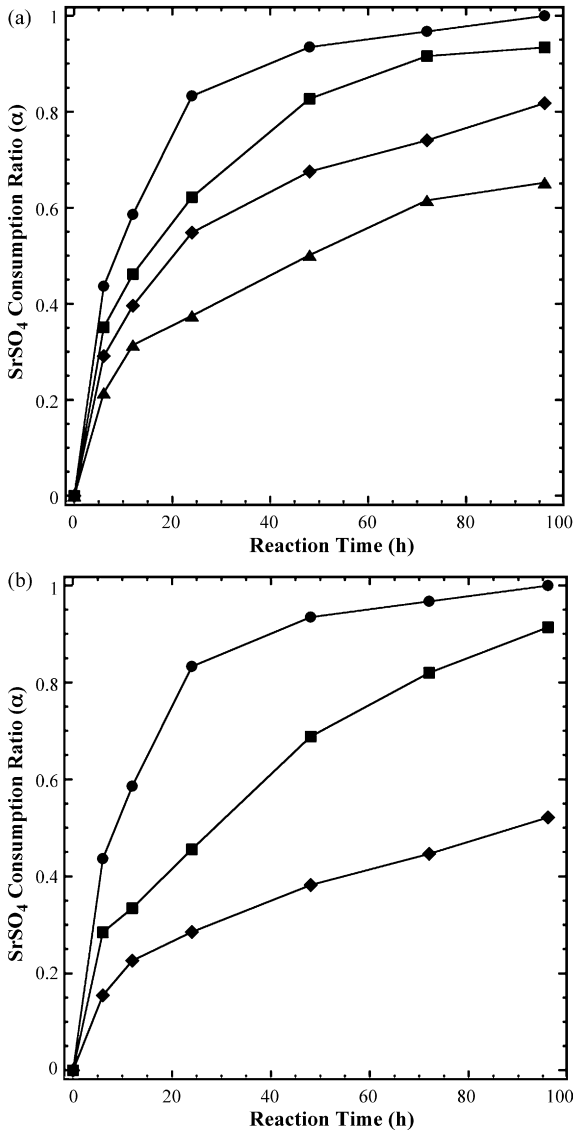

Fig. 9. Consumption ratio (α) curves determined for $SrSO_4$ crystal plates partially and completely transformed into $SrTiO_3$ powder under hydrothermal conditions, (a) in a 5 M KOH solution at temperatures of (▲) 150 °C, (♦) 175 °C, (■) 200 °C and (●) 250 °C; and (b) at 250 °C in different KOH solutions with concentrations of (♦) 1 M, (■) 2.5 M and (●) 5 M. All the treatments were conducted with an autoclave filling ratio of 40 % for several reaction intervals, respectively.

the precipitation of $SrTiO_3$ powders. Therefore, the data were fitted the first order kinetic function ($-\ln(1-\alpha) = kt$), because high correlation coefficient R^2 values (0.97–0.99) were obtained in comparison with those values calculated for other models, which also are functions employed to estimate the kinetics of solid–liquid chemical reactions, $1-(1-\alpha)^{1/3} = kt$ [21]. In addition, the constant rates determined by linear regression were used to calculate the activation energy "E_a" required for the transformation of $SrSO_4$ crystal into $SrTiO_3$ powders under alkaline hydrothermal conditions. The "E_a" value obtained from the Arrhenius plot equation was 27.9 kJ mol^{-1}; this value indicates that the one-step $SrTiO_3$ synthesis is a chemical reaction controlled process. And this value is similar to that determined for the synthesis of $BaTiO_3$ powders obtained under chemical reactions in the liquid state [38]. Although kinetic data regarding the consumption of $SrSO_4$ powders were difficult to determine in our case compared with those for $SrSO_4$ crystals, based on the X-ray diffraction results, we surmise that the kinetics of solid dissolution of the $SrSO_4$ powder should be accelerated by some magnitude orders and the activation energy value must be reduced as well.

The differences on the chemical kinetics might be due to the variation on the reactivity of both $SrSO_4$ and Ti-gel in the KOH solution under hydrothermal conditions, because this factor has a marked influence on the $SrSO_4$ dissolution rate and the saturation rate of the hydrothermal solution. Indeed, the dissolution is limited by a low chemical reactivity of the $SrSO_4$ crystals in contact with a high saturated 5 M KOH solution at low temperatures below 175 °C, and at 250 °C in low concentrated KOH solutions (1 or 2.5 M). In addition, the morphological aspects of the products obtained in this study revealed that the synthesis of $SrTiO_3$ particles proceeds by a massive bulk solid dissolution of the $SrSO_4$ and Ti gel.

4. Conclusions

In the present work, the feasibility for using low grade Sr^{2+} source reagent was investigated. The $SrSO_4$ mineral employed has demonstrated to exhibit an appropriate chemical reactivity for promoting the synthesis of $SrTiO_3$ powders under alkaline hydrothermal conditions, similar to that observed when using high purity expensive chemical reagents. Thus, celestite ($SrSO_4$) crystals were reacted in a single step into $SrTiO_3$ powder under hydrothermal conditions at 250 °C in a 5 M KOH solution, and this process was found to be completed after 96 h of treatment. Under these conditions, the synthesis of $SrTiO_3$ particles is mainly achieved by a coupled bulk dissolution–precipitation mechanism of ionic species, which was significantly affected by the chemical reactivity of the $SrSO_4$ crystal rather than by that of the Ti-gel in the alkaline (KOH) solvent hydrothermal media. Thus, the $SrTiO_3$ particles of micron size (0.5–15 μm) with two different morphologies, one of them peanut-like and the other one pseudocubic shapes, were produced as a result of the direct conversion. Kinetic data determined for the single-step synthesis of $SrTiO_3$ powders from precursor $SrSO_4$ crystals over a wide range of temperatures, indicate that the minimum activation energy required for this chemical reaction is 27.9 kJ mol^{-1}.

The synthesis of $SrTiO_3$ particles was remarkably accelerated by using $SrSO_4$ powder (size 25–38 μm), and was completed at 250 °C in 5 M KOH for 24 h. This result also suggested that the dissolution of $SrSO_4$ was important for the $SrTiO_3$ synthesis process. Fine pseudospherical $SrTiO_3$ particles with an average particle size of 0.4 μm were obtained from $SrSO_4$ powder by homogeneous formation of $SrTiO_3$ cubic particles followed by their dissolution and recrystallization.

Acknowledgments

This work was supported by the Coahuila State research grant FOMIX-COAH 2003-C02-02. Two of the authors, J.C.R.A. and Y.M.R.H., are indebted to CONACYT, Mexico, for financial support in the form of a Sabbatical research grant and a PhD scholarship to conduct part of this work, respectively. Many thanks are also given to MSc. Martha Rivas Aguilar, from CINVESTAV – Saltillo, México, for the Scanning Electron Microscopy observations.

References

[1] G.H. Haertling, Ferroelectric ceramics: history and technology, J. Am. Ceram. Soc. 82 (4) (1999) 797–818.
[2] V.V. Srdic, R.R. Djenadic, Nanocrystalline titanate powders: synthesis and mechanisms of perovskite particles formation, J. Optoelectron. Adv. Mater. 7 (6) (2005) 3005–3013.
[3] W.L. Suchanekhttp, M. Yoshimura, Preparation strontium titanate thin films by the hydrothermal–electrochemical method in a solution flow system, J. Am. Ceram. Soc. 81 (11) (1998) 2864–2868.
[4] M. Xu, Y.N. Lu, Y.F. Liu, S.Z. Shi, F. Fang, Synthesis of monosized strontium titanate particles with tailored morphologies, J. Am. Ceram. Soc. 89 (12) (2006) 3631–3634.
[5] D. Chen, X. Jiao, M. Zhang, Hydrothermal synthesis of strontium titanate powders with nanometer size derived from different precursors, J. Eur. Ceram. Soc. 20 (2000) 1261–1265.
[6] P.P. Phule, S.H. Risbud, Low-temperature synthesis and processing of electronic materials in the $BaO–TiO_2$ system, J. Mater. Sci. 25 (1990) 1169–1183.
[7] P.K. Gallagher, F. Schrey, F.V. Dimarcello, Preparation of semiconducting titanates by chemical methods, J. Am. Ceram. Soc. 46 (8) (1963) 359–365.
[8] J. Poth, R. Haberkorn, H.P.H.P. Beck, Combustion—synthesis of $SrTiO_3$. Part 1. Synthesis and properties of the ignition products, J. Eur. Ceram. Soc. 20 (2000) 707–713.
[9] R.M. Piticescu, P. Vilarnho, L.M. Popescu, R.R. Piticescu, Hydrothermal synthesis of perovskite based materials for microelectronic applications, J. Optoelectron Adv. Mater. 8 (2) (2006) 543–547.
[10] R. Wendelbo, D.E. Akporiaye, A. Karlsson, M. Plassen, A. Olafsen, Combinatorial hydrothermal synthesis and characterization of perovskites, J. Eur. Ceram. Soc. 26 (2006) 849–859.
[11] Y. Mao, S. Banerjee, S.S. Wong, Hydrothermal synthesis of perovskite nanotubes, Chem. Commun. (2003) 408–409.
[12] W.D. Yang, C.S. Hsieh, Fractional factorial design applied to optimize experimental conditions for preparation of ultrafine lanthanum-doped strontium titanate powders, J. Mater. Res. 14 (1999) 3410–3416.
[13] F.A. Rabuffetti, H.S. Kim, J.A. Enterkin, Y. Wang, C.H. Lanier, L.D. Marks, K.R. Poeppelmeier, P.C. Stair, Synthesis-dependent first-order Raman scattering in $SrTiO_3$ nanocubes at room temperature, Chem. Mater. 20 (2008) 5628–5635.
[14] S. Zhang, J. Liu, Y. Han, B. Chen, X. Li, Formation mechanism of $SrTiO_3$ nanoparticles under hydrothermal conditions, Mater. Sci. Eng. B 110 (2004) 11–17.
[15] X. Wei, G. Xu, Z. Ren, C. Xu, G. Shem, G. Han, PVA-assisted hydrothermal synthesis of $SrTiO_3$ nanoparticles with enhanced photocatalytic activity for degradation of RhB, J. Am. Ceram. Soc. 91 (11) (2008) 3795–3799.
[16] S. Zhang, Y. Han, B. Chen, X. Song, The influence of $TiO_2 \cdot H_2O$ gel on hydrothermal synthesis of $SrTiO_3$ powders, Mater. Lett. 51 (2001) 368–370.
[17] J.Y. Choi, C.H. Kim, D.K. Kim, Hydrothermal synthesis of spherical perovskite oxide powders using spherical gel powders, J. Am. Ceram. Soc. 81 (5) (1998) 1353–1356.
[18] R. Suárez-Orduña, J.C. Rendón-Angeles, J. López-Cuevas, K. Yanagisawa, The conversión of mineral celestite to strontianite under alkaline hydrothermal conditions, J. Sci. Phys: Condens. Matter. 16 (2004) S1331–S1344.
[19] R. Suárez-Orduña, J.C. Rendón-Angeles, Z. Matamoros-Veloza, K. Yanagisawa, Exchange of SO_4^{2-} ions with F^- ions in mineral celestite under hydrothermal conditions, Solid State Ionics 172 (2004) 393–396.
[20] M.M. Hessien, M.M. Hassan, K. El-Barawy, Synthesis and magnetic properties of strontium hexaferrite from celestite ore, J. Alloy Compd. 476 (2009) 373–378.
[21] H. Markus, S. Fugleberg, D. Valtakari, T. Salmi, D.Y. Murzin, M. Lahtinen, Kinetic modeling of a solid–liquid reaction: reduction of ferric iron to ferrous iron with zinc sulphide, Chem. Eng. Sci. 59 (2004) 919–930.
[22] S. Aydogan, A. Aras, M. Canbazoglu, Dissolution kinetics of sphalerite in acidic ferric chloride leaching, Chem. Eng. J. 114 (2005) 67–72.
[23] C.R. Peterson, E.B. Slamovich, Effect of processing parameter on the morphology of hydrothermally derived $PbTiO_3$ powders, J. Am. Ceram. Soc. 82 (7) (1999) 1702–1710.
[24] J. Moon, J.A. Kerchner, H. Krarup, J.H. Adaira, Hydrothermal synthesis of ferroelectric perovskites from chemically modified titanium isopropoxide and acetate salts, J. Mater. Res. 14 (2) (1999) 425–434.
[25] X. Wei, G. Xu, Z. Ren, G. Shen, G. Han, Effect of KOH concentration on the phase and morphology of hydrothermally synthesized $Pb_{0.70}La_{0.30}TiO_3$ powders, Mater. Lett. 62 (2008) 3719–3721.
[26] J. Moon, E. Suvaci, A. Morrone, S.A. Costantino, J.H. Adair, Formation mechanisms and morphological changes during the hydrothermal synthesis of $BaTiO_3$ particles from chemically modified, amorphous titanium (hydrous) oxide precursor, J. Eur. Ceram. Soc. 23 (2003) 2153–2161.

[27] J.C. Rendón-Angeles, Y.M. Rangel-Hernández, J. López-Cuevas, Z. Matamoros-Veloza, K. Yanagisawa, Pseudomorphic conversion of mineral $SrSO_4$ to $SrCrO_4$ under hydrothermal conditions, Joint Proceedings of the 20th AIRAPT-43rd EHPRG Conference on Science and Technology of High Pressure, Forschungszentrum Karlsruhe GmbH (Eds.), Karlsruhe Germany, ISBN 3-923704-49-6, Paper O144, 2005, 1–10.
[28] J.O. Eckert, C.C. Hung-Houston, B.L. Gersten, M.M. Lencka, R.E. Riman, Kinetics and mechanism of hydrothermal synthesis of barium titanate, J. Am. Ceram. Soc. 89 (11) (1996) 2929–2939.
[29] H. Xu, L. Gao, New evidence of a dissolution-precipitation mechanism in hydrothermal synthesis of barium titanate, Mater. Lett. 57 (2002) 490–494.
[30] S. Zhang, J. Liu, Y. Han, B. Chen, X. Li, Formation mechanisms of $SrTiO_3$ nanoparticles under hydrothermal conditions, Mater. Sci. Eng. B 110 (2004) 11–17.
[31] W. Hertl, Kinetics of barium titanate synthesis, J. Am. Ceram. Soc. 71 (10) (1998) 879–893.
[32] Y. Wang, L. Yang, Z. Ren, X. Wei, W. Weng, P. Du, G. Sheng, G. Han, Formation of single-crystal $SrTiO_3$ denditric nanostructures via simple hydrothermal method, J. Cryst. Growth 311 (2009) 2519–2523.
[33] J.C. Rendón-Angeles, M.I. Pech-Canul, J. López-Cuevas, Z. Matamoros-Veloza, K. Yanagisawa, Differences on the conversion of celestite in solutions bearing monovalent ions under hydrothermal conditions, J. Solid State Chem. 179 (2006) 3659–3666.
[34] M.M. Lencka, R.E. Riman, Thermodynamics of the hydrothermal synthesis of calcium titanate with reference to other alkaline-earth titanates, Chem. Mater. 7 (1) (1995) 17–25.
[35] M.M. Lencka, R.E. Riman, Thermodynamic modeling of hydrothermal synthesis of ceramic powders, Chem. Mater. 5 (1) (1993) 61–70.
[36] R.I. Walton, F. Millange, R.I. Smith, T.C. Hasen, D. O'hare, Real time observation of the hydrothermal crystallization of barium titanate using in situ neutron powder diffraction, J. Am. Chem. Soc. 123 (2001) 12547–12555.
[37] A. Testino, V. Buscagalia, M.t. Buscaglia, P. Nanni, Kinetic modeling of aqueous and hydrothermal synthesis of barium titanate ($BaTiO_3$), Chem. Mater. 17 (21) (2005) 5346–5356.
[38] M. Yoshimura, Powder-less processing for nano-structured bulk ceramics: realization of direct fabrication from solutions and/or melts, J. Ceram. Soc. Jpn. 114 (2006) 888–895.